Supplementary Information for Quantum Anharmonic Phonon Thermodynamics from the Free Energy Cumulant Expansion

Ethan J. Meitz[1], Aloïs Castellano[2], Gerald J. Wang[*3], and Alan J. H. McGaughey[†1]

[1]Department of Mechanical Engineering, Carnegie Mellon University, Pittsburgh, PA 15213, USA
[2]Q-MAT Research Center and European Theoretical Spectroscopy Facility, Université de Liège, Liège, Belgium
[3]Department of Civil and Environmental Engineering, Carnegie Mellon University, Pittsburgh, PA 15213, USA

[*]Corresponding author: gjwang@cmu.edu
[†]Corresponding author: mcgaughey@cmu.edu

S1 Estimating Derivatives of V_0

In this section, we derive the harmonic ensemble covariance estimator [Eq. (9)] used to compute temperature derivatives of the reference potential energy V_0 [Eq. (8)]. Let $\boldsymbol{q}$ denote the mass-normalized harmonic normal mode coordinates. Given harmonic interatomic force constants (IFCs), the harmonic probability density $p(\boldsymbol{q}, T)$, defines the likelihood of finding the phonons with amplitudes $\boldsymbol{q}$ at temperature T. At the harmonic level of theory, phonons are non-interacting and the probability density function is a product of independent Gaussian distributions,

$$p(\mathbf{q}, T) = \prod_i \frac{1}{\sqrt{2\pi\sigma_i^2(T)}} \exp\left[-\frac{q_i^2}{2\sigma_i^2(T)}\right], \qquad \sigma_i^2(T) \equiv \left\langle q_i^2 \right\rangle_{\mathrm{H}}. \tag{S1}$$

where σ_i^2 is the temperature dependent variance associated with phonon mode i. For an observable $A(\boldsymbol{q})$ with no explicit temperature dependence,

$$\frac{d}{dT}\left\langle A \right\rangle_{\mathrm{H}} = \int A(\mathbf{q})\, \partial_T p(\mathbf{q}, T)\, d\mathbf{q} = \left\langle A\, \partial_T \ln p(\mathbf{q}, T) \right\rangle_{\mathrm{H}}. \tag{S2}$$

Here $\langle\cdot\rangle_{\mathrm{H}}$ denotes an ensemble average where the Boltzmann weights are defined by the harmonic Hamiltonian. Eq. (S2) can be written as a covariance,

$$\frac{d}{dT}\left\langle A \right\rangle_{\mathrm{H}} = \mathrm{cov}_{\mathrm{H}}(A, \partial_T \ln(p(\mathbf{q}, T))), \qquad \mathrm{cov}_{\mathrm{H}}(A, B) = \left\langle AB \right\rangle_{\mathrm{H}} - \left\langle A \right\rangle_{\mathrm{H}} \left\langle B \right\rangle_{\mathrm{H}}. \tag{S3}$$

This is possible because $\langle \partial_T \ln p \rangle_{\mathrm{H}} = 0$ so the $\langle A \rangle_{\mathrm{H}} \langle B \rangle_{\mathrm{H}}$ term drops out. Taking the derivative of the log of the probability density gives us

$$\partial_T \ln(p(\mathbf{q}, T)) = \frac{1}{2} \sum_i \left[\frac{q_i^2}{\sigma_i^2(T)} - 1\right] \partial_T \ln \sigma_i^2(T), \tag{S4}$$

which we can plug into Eq. (S3) to find that

$$\frac{d}{dT}\left\langle A \right\rangle_{\mathrm{H}} = \frac{1}{k_{\mathrm{B}}T^2} \mathrm{cov}_{\mathrm{H}}\left(A, \widetilde{V}_2\right), \tag{S5}$$

where the effective harmonic energy, $\widetilde{V}_2$, is

$$\widetilde{V}_2(\mathbf{q}; T) \equiv \frac{k_{\mathrm{B}}T^2}{2} \sum_i \left(\partial_T \ln \sigma_i^2(T)\right) \frac{q_i^2}{\sigma_i^2(T)}. \tag{S6}$$

For a quantum harmonic oscillator in mass-normalized coordinates [1],

$$\sigma_i^2(T) = \frac{\hbar}{2\omega_i}\left[2n_i(T) + 1\right], \qquad n_i(T) = \frac{1}{\exp(\beta\hbar\omega_i) - 1}. \tag{S7}$$

where ω_i is the angular frequency of phonon mode i. When that frequency is independent of temperature or the envelope theorem applies (see Sec S2)

$$\partial_T n_i = \frac{\hbar\omega_i}{k_{\mathrm{B}}T^2} n_i(n_i + 1), \qquad \frac{k_{\mathrm{B}}T^2}{2} \partial_T \ln \sigma_i^2(T) = \frac{\hbar\omega_i n_i(n_i + 1)}{2n_i + 1}. \tag{S8}$$

Substituting Eq. (S8) into Eq. (S6) gives

$$\widetilde{V}_2(\mathbf{q}; T) = \frac{1}{2} \sum_i \frac{4n_i(T)\left[n_i(T) + 1\right]}{\left[2n_i(T) + 1\right]^2} \omega_i^2 q_i^2. \tag{S9}$$

The effective harmonic energy, $\widetilde{V}_2$, depends explicitly on temperature through the occupation numbers. When computing heat capacity we must differentiate $\widetilde{V}_2$. Taking the derivative treating only the occupation numbers as temperature dependent we obtain:

$$\frac{\partial \widetilde{V}_2}{\partial T} = \frac{1}{2} \sum_i \frac{4\hbar\omega_i}{k_{\mathrm{B}} T^2} \frac{n_i(n_i+1)}{(2n_i+1)^3} \omega_i^2 q_i^2. \tag{S10}$$

In the classical limit, $\widetilde{V}_2 = V_2$ and $\partial_T \widetilde{V}_2 = 0$ when the harmonic IFCs are held fixed.

S2 Importance of Self-Consistent Phonons

From the Gibbs–Bogoliubov inequality, the free energy of a trial harmonic system provides an upper bound to the exact free energy [2]. As shown in Sec. S3, sTDEP is equivalent to the stochastic self-consistent harmonic approximation (SSCHA), and therefore the sTDEP free energy, $\mathcal{F}^{\mathrm{sTDEP}}$, satisfies

$$\mathcal{F}^{\mathrm{sTDEP}} \geq \mathcal{F}. \tag{S11}$$

Accordingly, we choose the sTDEP/SSCHA harmonic IFCs, $\mathbf{\Phi}$, to minimize this upper bound on the exact free energy,

$$\mathbf{\Phi}^{\star}(T) \equiv \mathbf{\Phi}^{\mathrm{sTDEP}}(T) = \arg\min_{\mathbf{\Phi}} \mathcal{F}^{\mathrm{sTDEP}}[\mathbf{\Phi}, T]. \tag{S12}$$

This fact guarantees that the sTDEP IFCs define the optimal harmonic reference for approximating the exact free energy. We then define the minimized sTDEP free energy as

$$\mathcal{F}^{\mathrm{sTDEP}}(T) \equiv \mathcal{F}^{\mathrm{sTDEP}}[\mathbf{\Phi}^{\star}(T), T]. \tag{S13}$$

By the envelope theorem, the total derivative of the sTDEP free energy with respect to temperature is [3]

$$\frac{d\mathcal{F}^{\mathrm{sTDEP}}}{dT} = \left.\frac{\partial \mathcal{F}^{\mathrm{sTDEP}}}{\partial T}\right|_{\mathbf{\Phi}^{\star}(T)}. \tag{S14}$$

There are no derivatives with respect to $\mathbf{\Phi}$ due to the stationarity condition

$$\left.\frac{\partial \mathcal{F}^{\mathrm{sTDEP}}}{\partial \mathbf{\Phi}}\right|_{\mathbf{\Phi}^{\star}(T)} = 0. \tag{S15}$$

Accordingly, the entropy associated with the variational sTDEP free energy is

$$S^{\mathrm{sTDEP}} = -\frac{d\mathcal{F}^{\mathrm{sTDEP}}}{dT}, \tag{S16}$$

and requires no $\partial\omega/\partial T$ terms. This argument does not generally extend to the heat capacity, since second derivatives reintroduce terms involving $d\mathbf{\Phi}^{\star}/dT$. Likewise, it does not apply to higher-order corrections such as $\mathcal{F}_1$ and $\mathcal{F}_2$, since these terms are not part of the variational functional whose stationarity defines $\mathbf{\Phi}^{\star}$. That said, the use of sTDEP phonons, which satisfy Eq. (S12), reduces the number of neglected derivatives when computing entropy, internal energy, and heat capacity.

S3 sTDEP and SSCHA Equivalence

We will show that stochastic TDEP (sTDEP) is identical to the stochastic self-consistent harmonic approximation (SSCHA). Since the SSCHA IFCs minimize the Gibbs–Bogoliubov variational free-energy functional, it follows that the sTDEP IFCs satisfy the same variational bound [4]. In the SSCHA formalism, one introduces a family of trial density matrices and minimizes the corresponding free-energy functional over that family. We denote an arbitrary trial density matrix by ρ_k, where the subscript k labels a particular trial harmonic model (i.e., with trial harmonic IFCs Φ_k). The SSCHA free-energy is defined as [4]

$$\mathcal{F}^{\mathrm{SSCHA}}[\rho_k] = \langle K + V \rangle_k - T\mathcal{S}_k, \tag{S17}$$

where $\langle \cdot \rangle_k \equiv \mathrm{Tr}[\rho_k(\cdot)]$ denotes a quantum average with respect to ρ_k. For the trial labeled by k, we write the trial Hamiltonian,$\mathcal{H}_k$, as

$$\mathcal{H}_k = K + V_2^{(k)}, \tag{S18}$$

where $V_2^{(k)}$ is the harmonic trial potential associated with the auxiliary IFCs of trial k and K is the kinetic energy. Using this definition, the SSCHA free-energy functional, $\mathcal{F}^{\mathrm{SSCHA}}$, may be rewritten as

$$\begin{aligned} \mathcal{F}^{\mathrm{SSCHA}}[\rho_k] &= \langle K + V \rangle_k - T\mathcal{S}_k \\ &= \left\langle K + V - V_2^{(k)} + V_2^{(k)} \right\rangle_k - T\mathcal{S}_k \\ &= \left\langle K + V_2^{(k)} \right\rangle_k - T\mathcal{S}_k + \left\langle V - V_2^{(k)} \right\rangle_k . \end{aligned} \tag{S19}$$

Now define

$$\mathcal{F}_k \equiv \left\langle K + V_2^{(k)} \right\rangle_k - T\mathcal{S}_k, \tag{S20}$$

which is simply the Helmholtz free energy of the harmonic trial system generated by $\mathcal{H}_k$. Therefore,

$$\mathcal{F}^{\mathrm{SSCHA}} = \mathcal{F}_k + \left\langle V - V_2^{(k)} \right\rangle_k = \mathcal{F}^{\mathrm{sTDEP}}. \tag{S21}$$

The SSCHA and sTDEP IFCs differ only in notation and implementation. Thus, the sTDEP IFCs are also variationally optimal harmonic force constants, as they minimize the same free-energy functional as in the SSCHA.

S4 Cumulant Expansion Convergence Studies

S4.1 Size Effects

Size-effects only come into the calculation through the phonon-modes (i.e., ω and $\mathcal{F}_{\mathrm{H}}$). To remove size-effects the supercell only needs to be bigger than twice the cutoff-radius. As a sanity check, Figs. S1(a) - S1(d), show the effect of supercell size on the total free energy, entropy, internal energy, and heat capacity calculated from the cumulant expansion for LJ argon. Increasing the cell size changes the free energy and internal energy by less than 0.01 meV/atom. Likewise for entropy and heat capacity, the change is less than 0.1%. The variation results from the fact that the IFCs are fit independently for each supercell. Therefore, we use the $4 \times 4 \times 4$ supercell for LJ argon and LJ neon (256 atoms). For SW silicon we use a $3 \times 3 \times 3$ supercell for SW silicon (216 atoms), which was sufficient to negate size effects on the phonons in Ref. 5.

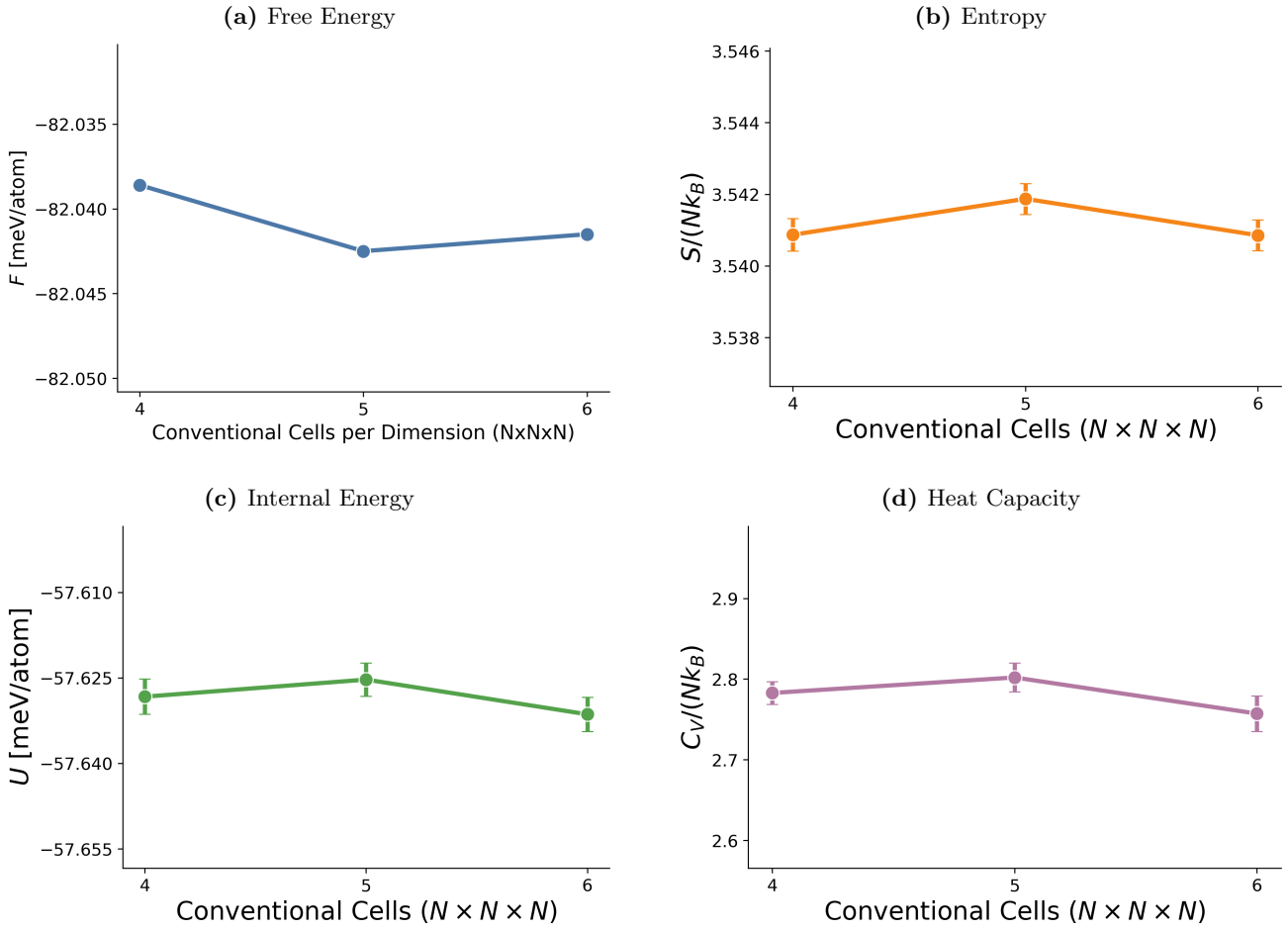

Figure S1: Size-effect analysis for the free energy, entropy, internal energy, and heat capacity of LJ Argon at 80K.

S4.2 Constant Corrections

The constant term for all thermodynamic properties converges within 100,000 samples at the maximum temperature studied for each material. For all materials in Figs. S2-S4, the free energy and internal energy are converged within 0.1 meV/atom and the variation in heat capacity and entropy is below 0.1%.

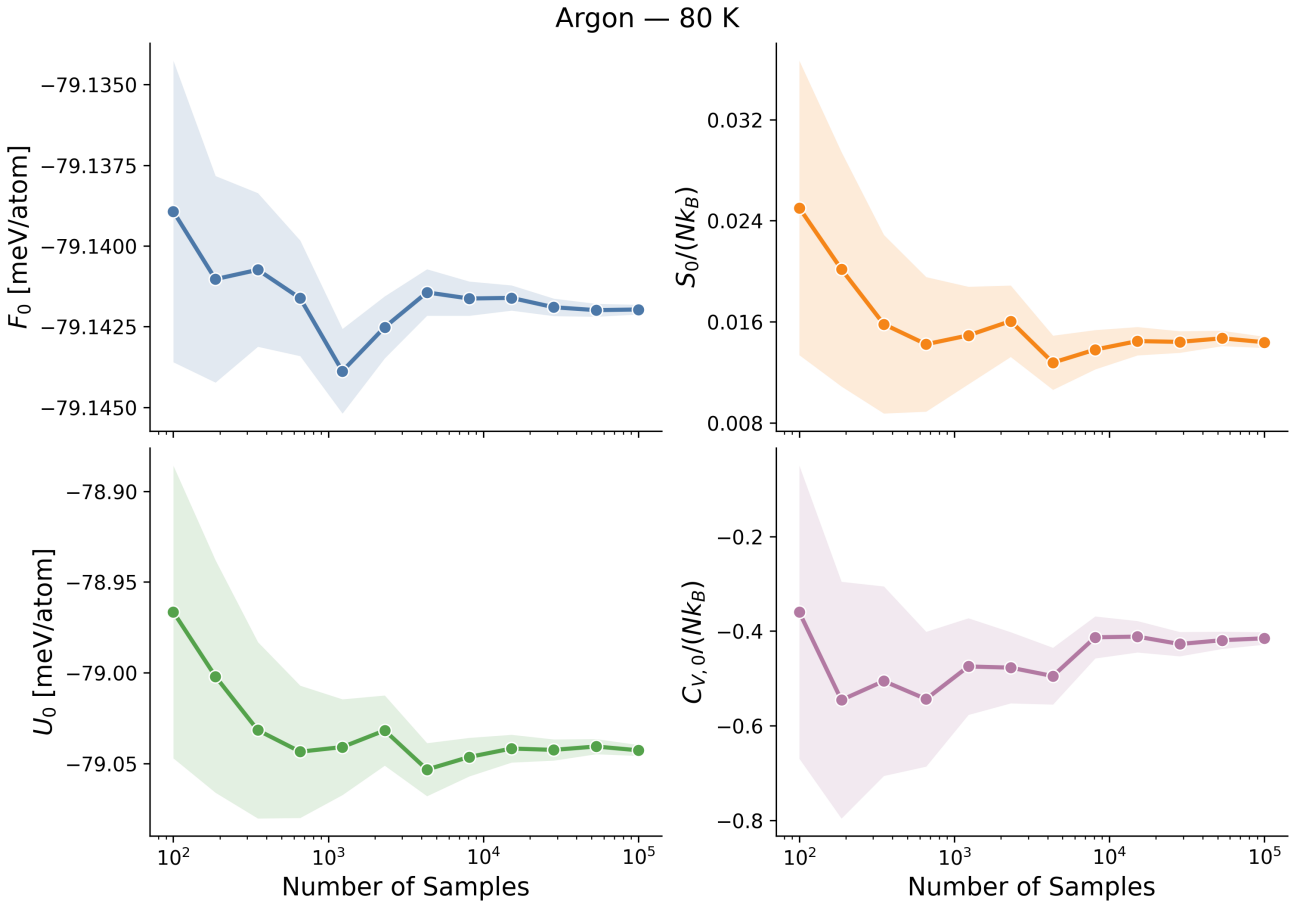

Figure S2: Convergence of the constant corrections for LJ argon at 80 K as a function of the number of samples. The shaded region represents one standard error estimated by bootstrapping.

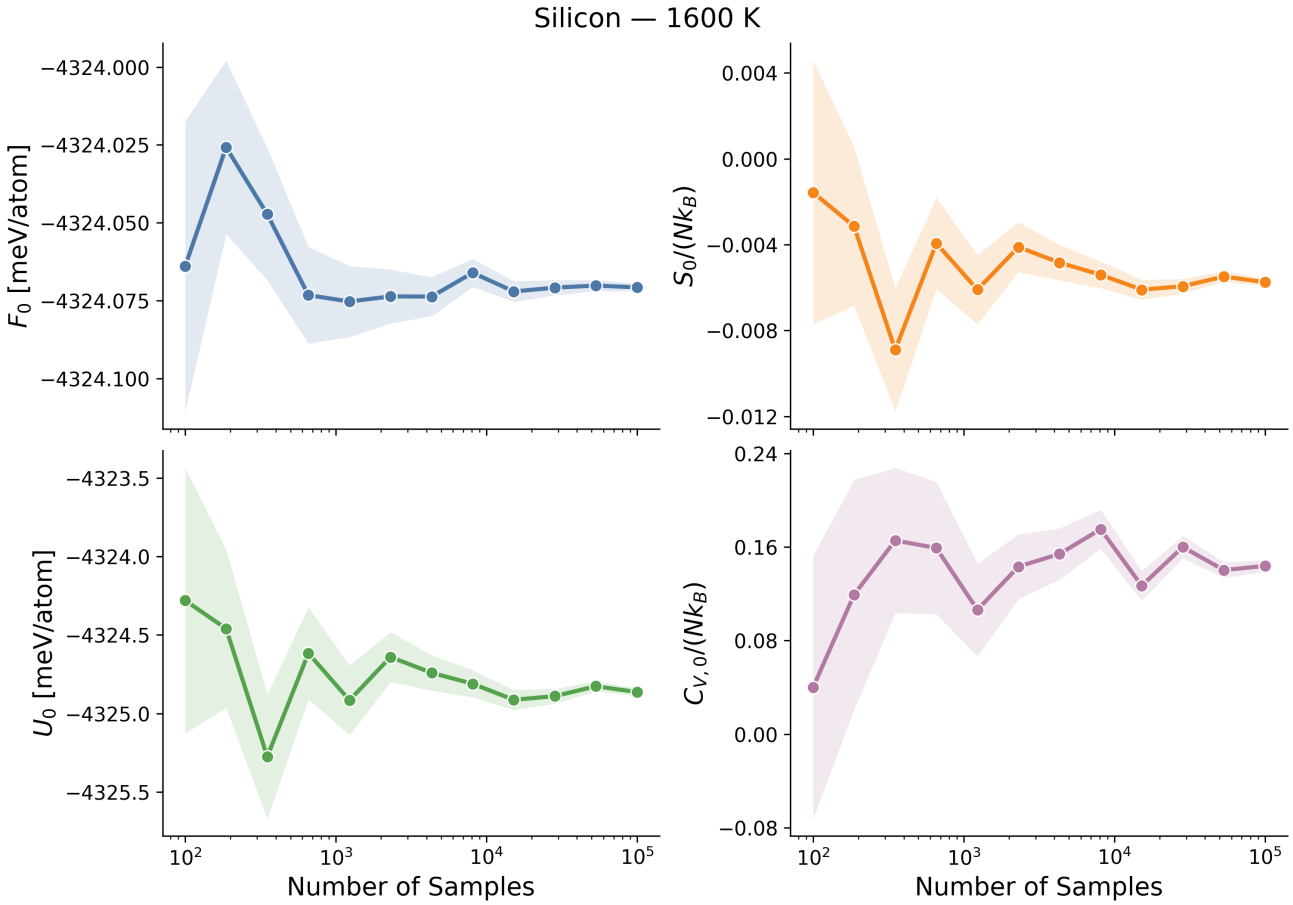

Figure S3: Convergence of the constant corrections for Stillinger-Weber silicon at 1600 K as a function of the number of samples. The shaded region represents one standard error estimated by bootstrapping.

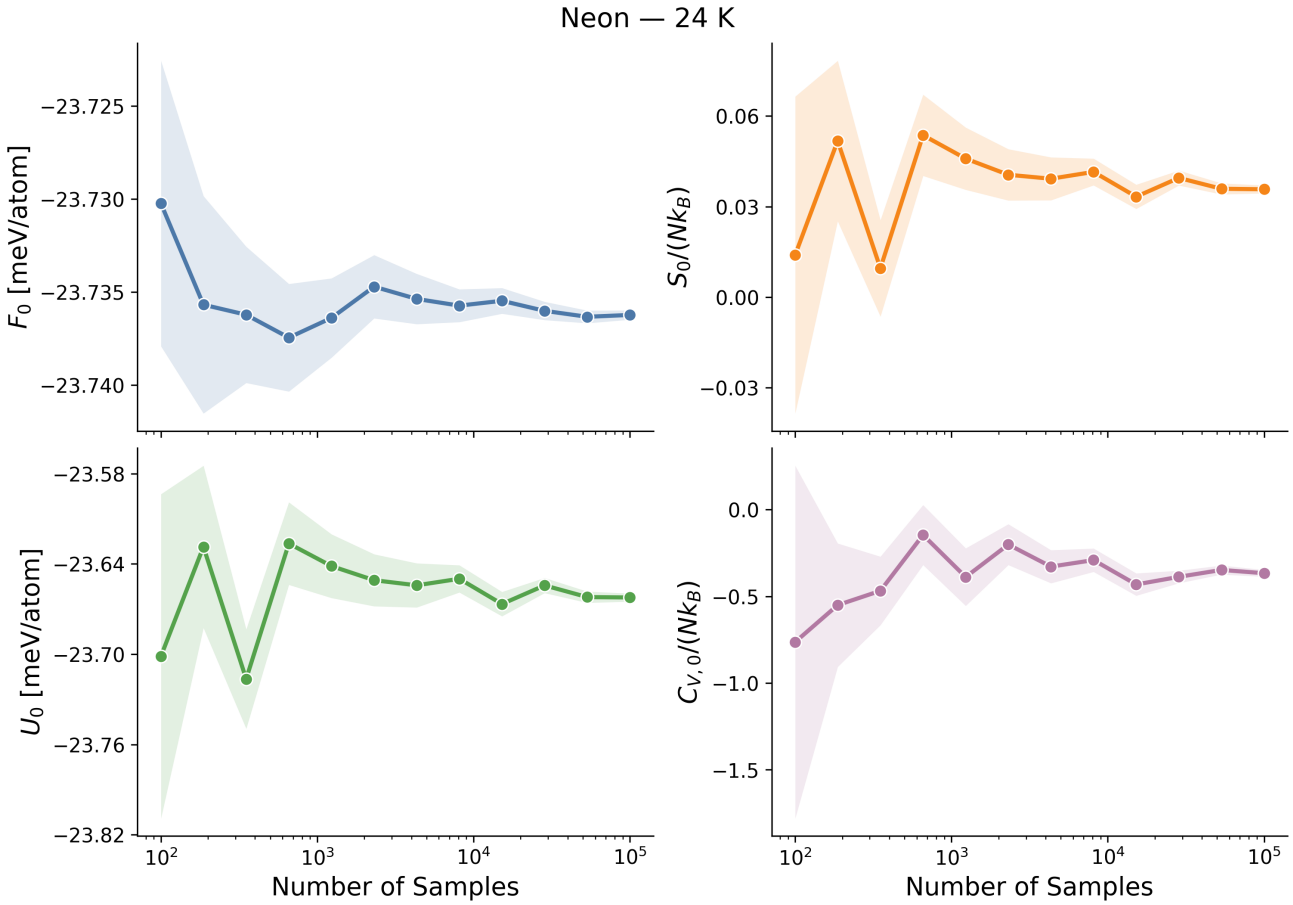

Figure S4: Convergence of the constant corrections for LJ neon at 24 K as a function of the number of samples. The shaded region represents one standard error estimated by bootstrapping.

S4.3 *k*-mesh Convergence of $\mathcal{F}_1$ and $\mathcal{F}_2$

We adopt a k-mesh of $25 \times 25 \times 25$ for all calculations. Figs. S5-S7 show that all materials are converged within 0.01 meV/atom at the minimum and maximum temperatures for free energy and internal energy. The entropy and heat capacity are likewise well converged with deviations below 0.1%.

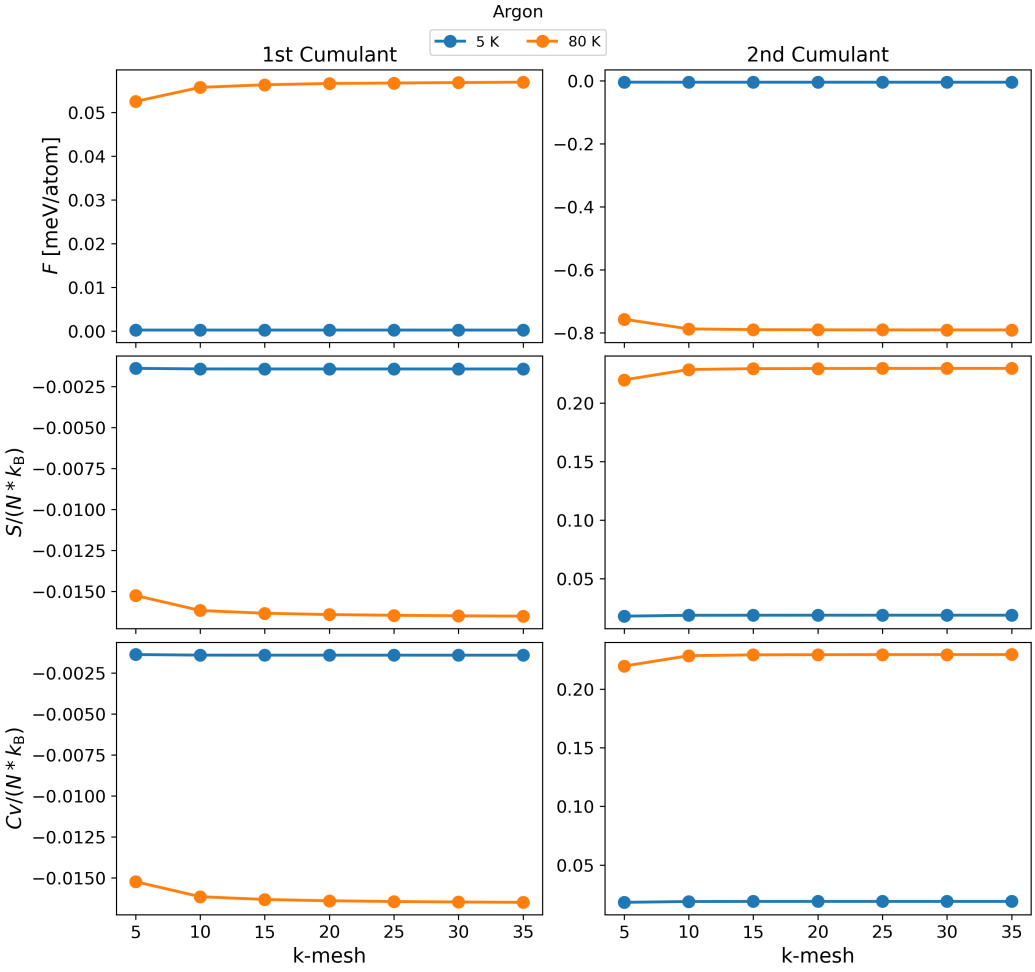

Figure S5: Convergence of $\mathcal{F}_1$ and $\mathcal{F}_2$ for LJ argon at 5 K and 80 K as a function of the k-mesh dimensions.

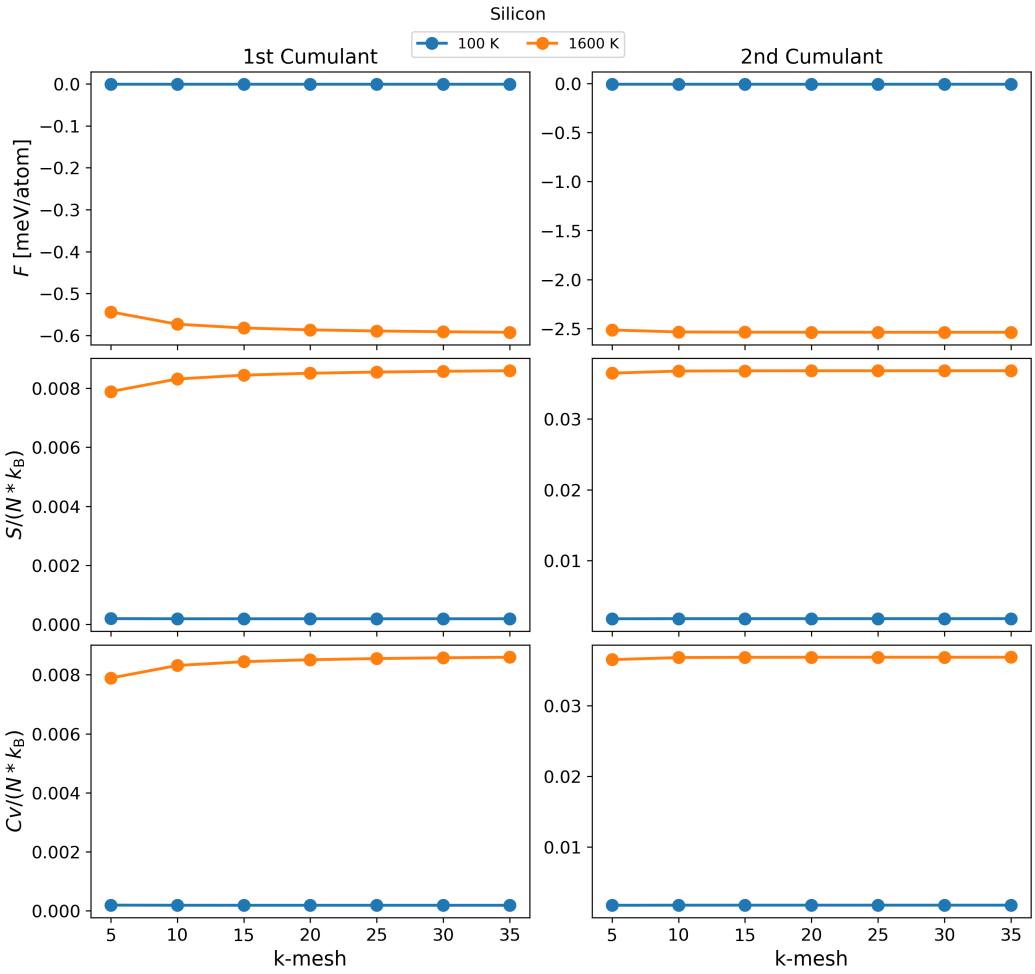

Figure S6: Convergence of $\mathcal{F}_1$ and $\mathcal{F}_2$ for Stillinger-Weber silicon at 100 K and 1600 K as a function of the k-mesh dimensions.

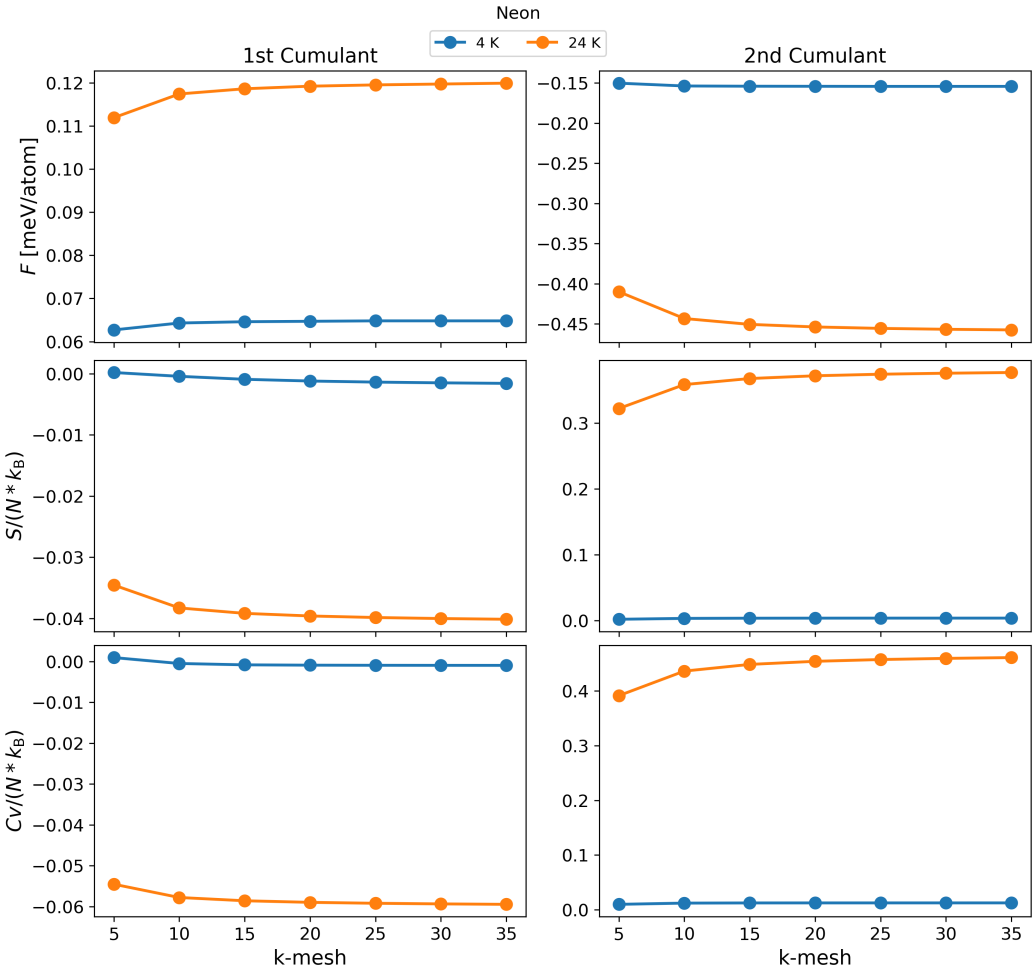

Figure S7: Convergence of $\mathcal{F}_1$ and $\mathcal{F}_2$ for LJ neon at 4 K and 24 K as a function of the k-mesh dimensions.

S5 PIMD Bead Convergence

Previous PIMD studies demonstrated that using $200/T$ beads for each temperature, T, was sufficient to converge the energy estimators as well as lattice constants for LJ neon [6]. However, we found that this relationship was insufficient for predicting accurate heat capacities when using the scaled-coordinates estimator [7]. To ensure that our heat capacity estimates were converged, we estimated heat capacity from 12–24 K using $400/T$, $300/T$, and $200/T$ to determine the number of beads. Each estimate was the average of 3 seeds with 50,000 data points sampled every 30 fs. For each temperature, we estimate the bias of the Trotter-Suzuki factorization used to estimate the path integrals in PIMD by fitting:

$$A(N_{\text{beads}}) = A_\infty + \frac{a}{N_{\text{beads}}^2} + \mathcal{O}\left(\frac{1}{N_{\text{beads}}^4}\right), \tag{S22}$$

where A is an arbitrary property measured from the PIMD simulation, N_{beads} is the number of beads, and A_∞ is the extrapolated infinite-bead limit. This leading N_{beads}^{-2} form is the expected convergence of the second-order Trotter–Suzuki discretization. From each fit we extract the intercept term, A_∞, and determine the minimum number of beads required to be within some tolerance of A_∞. For heat capacity, we used a tolerance of 1% of Dulong–Petit (0.03 Nk_{B}) and for internal energy, we chose 0.1 meV/atom. The internal energy tolerance was chosen to be small in order to check the original $200/T$ expression. The bead-convergence analysis gives the minimum number of beads for heat capacity and internal energy as a function of temperature with a function proportional to $1/T$ fit to the data. Figure S8 confirms that $200/T$ is sufficient to converge internal energy, but that $440/T$ is necessary for heat capacity. Due to the worse fit for heat capacity, we use $N_{\text{beads}} = 550/T$ to be conservative.

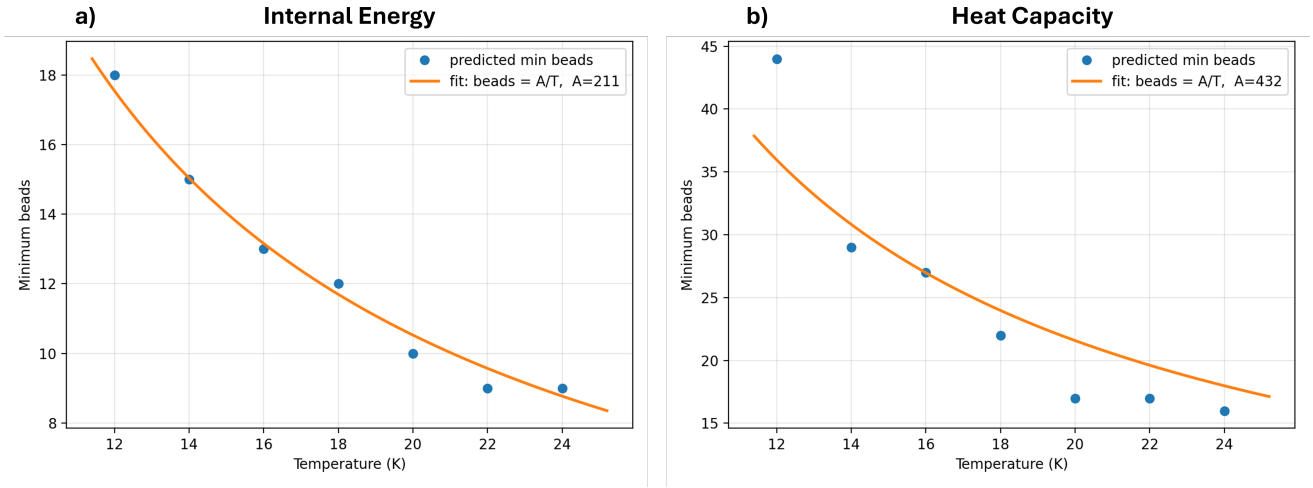

Figure S8: Minimum number of PIMD beads required to converge the (a) internal energy and (b) heat capacity as a function of temperature.

S6 Thermodynamic Integration Finite-Size Effects

The Einstein solid reference is susceptible to finite-size effects due to the low accuracy of the Einstein solid as a reference system [8]. To be sure that our reference free energies were accurate, we computed the free energy as a function of system size for both LJ argon and SW silicon. Fig. S9 shows that LJ argon converges at 10,976 atoms while SW silicon converges at 13,824 atoms.

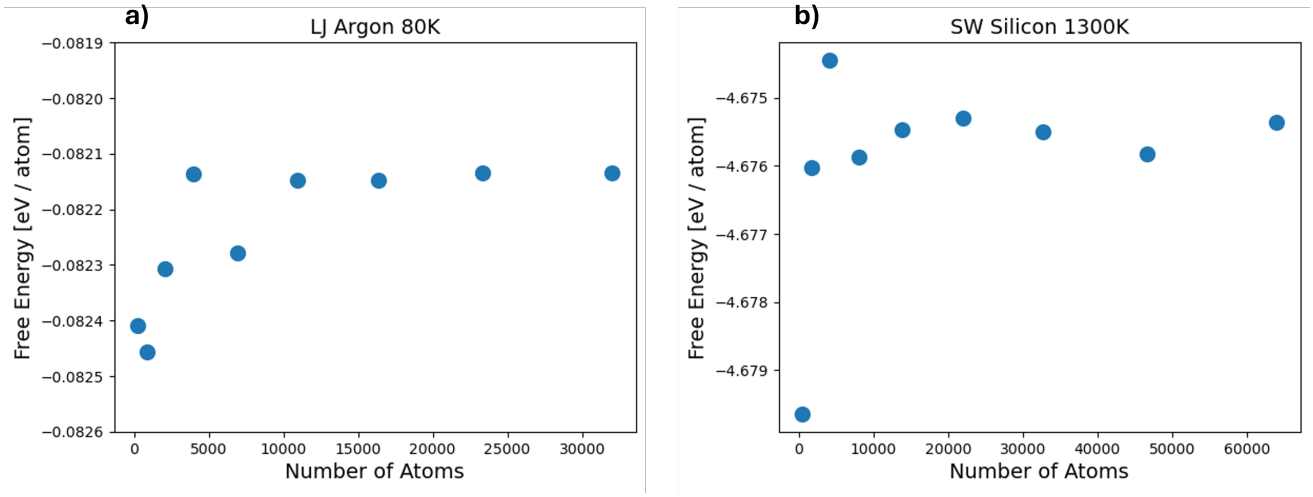

Figure S9: Effect of supercell size on the free energy for (a) LJ Argon at 80K and (b) SW silicon at 1300K

References

[1] Shulumba, N., Hellman, O. & Minnich, A. J. Intrinsic localized mode and low thermal conductivity of PbSe. *Physical Review B* **95**, 014302 (2017). URL https://link.aps.org/doi/10.1103/PhysRevB.95.014302.

[2] Feynman, R. P. *Statistical Mechanics: A Set Of Lectures* 0 edn (CRC Press, 2018). URL https://www.taylorfrancis.com/books/9780429961588.

[3] Milgrom, P. & Segal, I. Envelope Theorems for Arbitrary Choice Sets. *Econometrica* **70**, 583–601 (2002). URL http://doi.wiley.com/10.1111/1468-0262.00296.

[4] Monacelli, L. *et al.* The stochastic self-consistent harmonic approximation: calculating vibrational properties of materials with full quantum and anharmonic effects. *Journal of Physics: Condensed Matter* **33**, 363001 (2021). URL https://iopscience.iop.org/article/10.1088/1361-648X/ac066b.

[5] Meitz, E. J., Wang, G. J. & McGaughey, A. J. H. Phonon mode resolved anharmonic heat capacity of solids. *Physical Review B* **111**, 064305 (2025). URL https://link.aps.org/doi/10.1103/PhysRevB.111.064305.

[6] Herrero, C. P. & Ramírez, R. Path-integral simulation of solids. *Journal of Physics: Condensed Matter* **26**, 233201 (2014). URL https://iopscience.iop.org/article/10.1088/0953-8984/26/23/233201.

[7] Yamamoto, T. M. Path-integral virial estimator based on the scaling of fluctuation coordinates: Application to quantum clusters with fourth-order propagators. *The Journal of Chemical Physics* **123**, 104101 (2005). URL https://pubs.aip.org/jcp/article/123/10/104101/898475/Path-integral-virial-estimator-based-on-the.

[8] Freitas, R., Asta, M. & De Koning, M. Nonequilibrium free-energy calculation of solids using LAMMPS. *Computational Materials Science* **112**, 333–341 (2016). URL https://linkinghub.elsevier.com/retrieve/pii/S0927025615007089.